Molecular Therapy
Original Article

USP22 deficiency in melanoma mediates resistance to T cells through IFNγ-JAK1-STAT1 signal axis

Min Li,[1,2,4] Yanqin Xu,[1,2,4] Jie Liang,[1] Hao Lin,[1] Xinyue Qi,[1] Fanlin Li,[1] Ping Han,[1] Yanfeng Gao,[3] and Xuanming Yang[1,2]

[1]Sheng Yushou Center of Cell Biology and Immunology, School of Life Sciences and Biotechnology, Shanghai Jiao Tong University, Shanghai, People's Republic of China; [2]Joint International Research Laboratory of Metabolic & Developmental Sciences, Shanghai Jiao Tong University, Shanghai, People's Republic of China; [3]School of Pharmaceutical Sciences (Shenzhen), Sun Yat-sen University, Shenzhen, Guangdong, People's Republic of China

Genome-wide clustered regularly interspaced short palindromic repeats (CRISPR)-CRISPR-associated 9 (Cas9)-mediated loss-of-function screens are powerful tools for identifying genes responsible for diverse phenotypes. Here, we perturbed genes in melanoma cells to screen for genes involved in tumor escape from T cell-mediated killing. Multiple interferon gamma (IFNγ) signaling-related genes were enriched in melanoma cells resistant to T cell killing. In addition, deletion of the deubiquitinating protease ubiquitin specific peptidase 22 (USP22) in mouse melanoma (B16-OVA) cells decreased the efficacy of T cell-mediated killing, both *in vitro* and *in vivo*, while overexpression enhanced tumor-cell sensitivity to T (OT-I) cell-mediated killing. *USP22* deficiency in both mouse and human melanoma cells showed impaired sensitivity to interferon pathway and USP22 was positively correlated with key molecules of interferon pathway in clinical melanoma samples. Mechanistically, USP22 may directly interact with signal transducer and activator of transcription 1 (STAT1), deubiquitinate it, and improve its stability in both human and mouse melanoma cells. Our findings identified a previously unknown function of USP22 and linked the loss of genes in tumor cells that are essential for escaping the effector function of $CD8^+$ T cells during immunotherapy.

INTRODUCTION

Immune checkpoint-blocking antibodies against programmed death 1/programmed death-ligand 1 (PD-1/PD-L1) and cytotoxic T-lymphocyte-associated protein 4 (CTLA-4) are designed to reactivate tumor-specific T cells, which have demonstrated effectiveness against a large number of cancer types, including melanoma, non-small cell lung cancer, and renal cancer.[1–4] However, only 17%–26% of melanoma patients respond to anti-PD-L1 therapy,[5] and only 2%–6% respond to anti-CTLA-4 therapy.[2,5] Recently, multiple genes and pathways have been found to contribute to therapeutic resistance to cancer immunotherapy. Several interferon-pathway-related molecules have been identified involved in immunotherapy resistance. Tumor cells deficient in *Stat1*, *Jak1*, *Ifngr2*, *Ifngr1*, and *Jak2*, which are required for sensing and signaling through the interferon gamma (IFNγ) pathway, were significantly enriched after anti-PD-1 treatment.[6,7] On the contrast, tumor cells deficient in *Ptpn2*, *H2-T23*, *Ripk1*, and *Stub1* were significantly depleted, which are potential negative regulators of the IFN pathway. Ptpn2 decreases IFNγ sensing by tumor cells through the dephosphorylation of Janus kinase 1 (JAK1) and signal transducer and activator of transcription 1 (STAT1).[6,8,9] These studies highlight the comprehensive immune-escaping mechanisms utilized by tumor cells and the essential role of IFN pathway in regulating cancer immunotherapy.

Ubiquitin-specific protease 22 (USP22) is a member of the USP family, which is the subfamily of deubiquitinating proteases (DUBs).[10] USP22 is a human Spt-Ada-Gcn5-acetyltransferase (SAGA) complex subunit, which plays an important role in the histone acetylation through GCN5 and deubiquitination of histones H2B and H2A through USP22 and also takes part in regulating gene transcription.[11–13] USP22 is also reported to enhance sirtuin 1 (SIRT1) stability through its deubiquitination and negatively regulate STAT3 acetylation.[14] Multiple genes can be indirectly regulated by USP22 through SIRT1, such as *c-MYC*, *p53*, and *Gα12*.[13,15–17] Because USP22 is reported to be one of the 11 "death of cancer" genes,[18,19] much research on USP22 has mainly focused on its role in tumor cells.[20–22] USP22 is able to deubiquitinate cyclin B1 (CCNB1) to promote cell proliferation and tumorigenesis in colon cancer[23] and deubiquitinate lysine (K)-specific demethylase 1A (KDM1A) to promote tumorigenesis in glioblastoma.[24] High expression levels of USP22 are correlated with poor prognosis in various cancer types.[20–22,25–29] However, whether USP22 is able to affect the interaction between tumor cells and immune cells remains unclear.

Received 8 July 2020; accepted 11 February 2021;
https://doi.org/10.1016/j.ymthe.2021.02.018.

[4]These authors contributed equally

Correspondence: Xuanming Yang, Sheng Yushou Center of Cell Biology and Immunology, School of Life Sciences and Biotechnology, Shanghai Jiao Tong University, 800 Dongchuan Road, Shanghai 200240, People's Republic of China.
E-mail: xuanmingyang@sjtu.edu.cn

IFNγ transduces its activation signals through binding to the IFNγ receptor (IFNGR), which consists of the two subunits, IFNGR1 and IFNGR2. Binding of IFNγ to its receptor leads to the recruitment and activation of JAK1 and JAK2 and the subsequent phosphorylation, dimerization, and activation of the transcription factor STAT1. STAT1 homodimers then translocate to the nucleus, where they bind to specific promoter elements and modulate the transcription of IFNγ-regulated genes.[30] IFNγ is a key effector cytokine released from activated T cells after recognition of their target tumor cells. IFNγ exhibits multiple anti-tumor effects, including induction of apoptosis in tumor cells, inhibition of angiogenesis, and activation of immune cells.[30] IFNγ-pathway-related gene deficiency has been reported to cause resistance to immune checkpoint blockade therapy.[6,7,31]

Considering the essential role of $CD8^+$ T cells in anti-tumor immunity, we aimed to identify undiscovered mechanisms involved in resistance to T cell-mediated killing. Using clustered regularly interspaced short palindromic repeats (CRISPR)-CRISPR-associated 9 (Cas9) based whole-genome editing technology, we developed an *in vitro* and *in vivo* combined screening approach to identify genes involved in resistance to T cell-mediated killing. Using this approach, we determined that USP22 was able to deubiquitinate STAT1 to enhance its stability, which in turn regulated the sensitivity of tumor cells to T cells and IFNγ. Manipulating the activity of USP22 may open new directions into the design of combination therapies using adoptive transfer therapy.

RESULTS

Identification of USP22 by genome-wide CRISPR-Cas9 screening as a potential candidate regulator of resistance to T cell killing

T cells are one of the most important components of anti-tumor immunity;[32,33] however, evading immune responses is a hallmark of cancers.[34,35] To screen potential genes involved in T cell-killing resistance, we established a pool of stable genome-wide gene knockouts in B16-OVA cells, which are ovalbumin (OVA)-transfected clones derived from the murine melanoma cell line B16.[36] In this pool, the B16-OVA cells were transfected with the lentiviral GeCKOv2 library, which contains 130,209 unique single guide RNAs (sgRNAs) targeting 20,611 genes.[37] To facilitate the screening of tumor-specific T cell killing, OVA served as a specific model antigen. Overexpression enhanced tumor-cell sensitivity to T (OT-I) $CD8^+$ T cells are able to specifically recognize the $OVA_{257-264}$ peptide/H2-K^b complex.[38] We used OT-I T cells to screen for T cell-killing resistance-related genes using both *in vitro* co-culture assays and *in vivo* killing assays (Figure 1A). The remaining tumor cells were considered to be T cell-killing resistant clones. We quantified sgRNA abundance in these cells by deep sequencing of the amplified sgRNA cassettes. Among the sgRNAs, *Jak1*, which had been previously identified by other groups,[6,7] served as a positive control for our screening process. Among the sgRNAs identified in our current study, *USP22* ranked 1 and 7 *in vivo* and 13 and 247 *in vitro* from 4 independent screenings (Table S1). This suggested that *USP22* may be a potential candidate gene related with T cell-killing resistance. To confirm the T cell-killing resistance phenotype mediated by *USP22* deficiency, we established two B16-OVA-$USP22^{null}$ monoclonal cell lines using CRISPR-Cas9 targeting a different genome locus. Disruption of the *USP22* gene and protein expressions was verified by cDNA Sanger sequencing, flow cytometry, and whole-cell-lysate western blot analysis (Figure S1). The efficacy of adoptively transferred OT-I T cells against parental B16-OVA tumor cells and *USP22*-deficient B16-OVA-$USP22^{null}$ tumor cells was then tested *in vivo*. Both *USP22*-deficient clones demonstrated treatment-resistant phenotype to OT-I T cell adoptive transfer; however, the same treatment induced approximately 60%–80% tumor burden reduction in the parental B16-OVA tumors (Figures 1B–1D). To further investigate whether *USP22* deficiency could directly induce T cell-killing resistance, B16-OVA or B16-OVA-$USP22^{null}$ cells were co-cultured with OT-I T cells *in vitro*. Consistent with the *in vivo* phenotype, B16-OVA-$USP22^{null}$ cells were resistant to OT-I T cell-mediated killing *in vitro* (Figures 1E and S2). These data collectively suggested that USP22 directly affected the efficiency of T cell-mediated killing of tumor cells.

USP22 overexpression sensitized B16-OVA to T cell-mediated killing

The results described above demonstrated that USP22 loss-of-function in tumor cells induced resistance to T cell-mediated killing. Accordingly, we wondered whether USP22 gain-of-function would enhance the sensitivity of tumor cells to T cell-mediated cytotoxicity. To investigate this, we established USP22-overexpressing B16-OVA monoclonal stable cell lines. Compared with the parental B16-OVA cell line, the mRNA and protein expressional levels of USP22 were significantly higher in the two clones B16-OVA-$USP22^{high}$ #1 and B16-OVA-$USP22^{high}$ #16 (Figure S3). We then tested the efficacy of adoptively transferred OT-I T cells into B16-OVA and B16-OVA-$USP22^{high}$ tumor-bearing mice. The adoptive transfer of OT-I T cells significantly repressed tumor growth under conditions of both wild-type (WT) expression and overexpression of USP22 (Figures 2A–2C).

To further dissect whether USP22 overexpression could directly induce T cell-killing resistance, B16-OVA and B16-OVA-$USP22^{high}$ cells were co-cultured with OT-I T cells *in vitro*. Consistent with the *in vivo* phenotype, B16-OVA-$USP22^{high}$ cells were more sensitive to OT-I T cell-mediated killing *in vitro* compared to WT B16-OVA (Figure 2D). These results demonstrated that USP22 expression in tumor cells directly enhanced their sensitivity to T cell cytotoxicity.

Global RNA sequencing revealed that USP22 activity was associated with the IFN signaling pathway

To assess the genetic mechanisms underlying the functional properties of *USP22* knockout and overexpression in B16-OVA tumor cells, we compared the gene expression profiles with that of WT B16-OVA using whole-exome sequencing. We observed opposing gene expression patterns in the *USP22* knockout and overexpressing B16-OVA cells for the differentially expressed genes (Figure 3A; Table S2). These differences correlated well with the distinct T cell-killing resistance phenotypes of B16-OVA-$USP22^{null}$ and B16-OVA-$USP22^{high}$

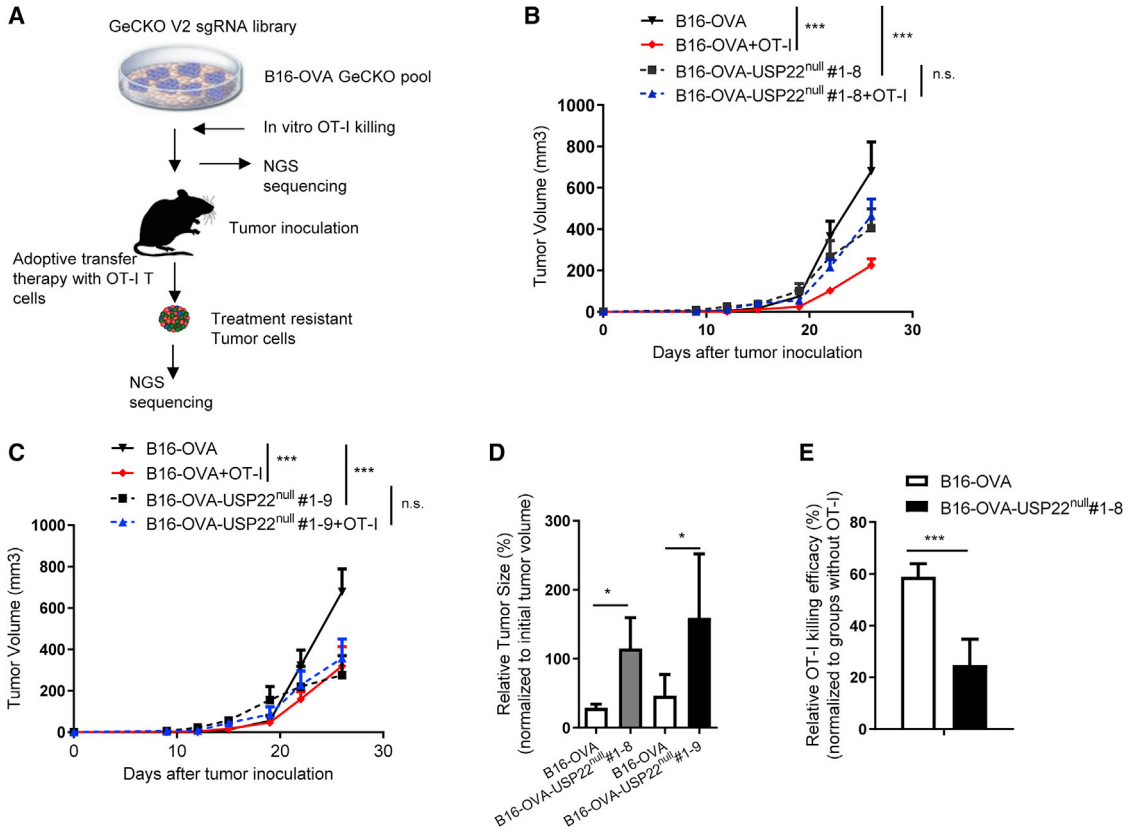

Figure 1. Identification of USP22 as a potential candidate regulator of tumor cell resistance to T cell killing

(A) Workflow of CRISPR-Cas9-based screening of potential genes associated with B16-OVA resistance to T cell killing. (B and C) Wild-type (WT) C57BL/6 mice (n = 6/group) were subcutaneously inoculated with B16-OVA, B16-OVA-USP22^{null} #1–8 (B), or B16-OVA-USP22^{null} #1–9 (C) cells; OT-I T cells were then administered on days 12 and 15 post-tumor-inoculation. Tumor size was measured twice a week. Data represent means ± SEM. (D) The relative tumor volume (the ratio of tumor volumes of OT-I T cell-treated groups compared to that of the control group) for engrafted B16-OVA cells, B16-OVA-USP22^{null} #1–8 cells, and B16-OVA-USP22^{null} #1–9 cells on day 27 post-transplantation are shown. (E) B16-OVA or B16-OVA-USP22^{null} #1–8 cells were cultured *in vitro* alone or with OT-I T cells for 3 days. The remaining tumor cells resistant to OT-I killing were quantified by counting the trypan-blue-negative cells (left panel). The relative *in vitro* killing efficiency (ratio of remaining tumor cells in the presence of OT-I T cells compared to that in the absence of OT-I T cells) is shown in the right panel. Data are shown as the mean ± SEM (B and C) or mean ± SD (D and E). *p < 0.05, ***p < 0.001. Representative results of one from two (B–D) or five (E) repeated experiments are shown.

cells. Using volcano plot analyses, we determined that multiple IFN-related genes were upregulated when USP22 was overexpressed (Figure 3B; Table S2). To further confirm this finding, we analyzed the gene expression levels of 11 representative IFN-related genes by quantitative polymerase chain reaction (qPCR). The expression level of all the genes was increased in the B16-OVA-USP22^{high} cells and decreased in the B16-OVA-USP22^{null} cells (Figure 3C). Furthermore, we observed similar positive correlation between the expression of USP22 and key molecules (IFNGR1, IFNGR2, JAK1, JAK2, and STAT1) of the IFN signaling pathway in primary human skin cutaneous melanoma patients (Figure 3D). These results suggested that USP22 positively regulated the IFN-related pathway. To investigate whether USP22 could enhance the activation strength of the IFN signaling pathway, we compared the levels of phosphorylation of STAT1, a key indicator of IFN-JAK-STAT activation.[39] Following IFNγ stimulation, phosphorylation of STAT1 increased in B16-OVA-USP22^{high} cells and decreased in B16-OVA-USP22^{null} cells. We also observed a background level of STAT1 phosphorylation in B16-OVA cells overexpressing USP22 (Figure 3E). These data demonstrated that USP22 was able to regulate the IFN-related pathway, which might have further impaired the sensitivity of the tumor cells to T cell-mediated killing.

T cell-killing resistance mediated by *USP22* deficiency was dependent on JAK1

We showed above that USP22 could sufficiently enhance the sensitivity of the IFN signaling pathway. However, it remained unclear whether this regulation was necessary for USP22-mediated resistance to T cell killing. To investigate this, we disrupted the IFN pathway by knocking out JAK1 expression in *USP22*-deficient and -overexpressing B16-OVA cells. The *Jak1* deficiency was confirmed by non-induced PD-L1 expression after IFNγ stimulation (Figure S4), similar to previous studies.[7] These cell lines were then co-cultured with OT-I T cells, and the efficiency of T cell killing was compared. B16-OVA-JAK1^{null},

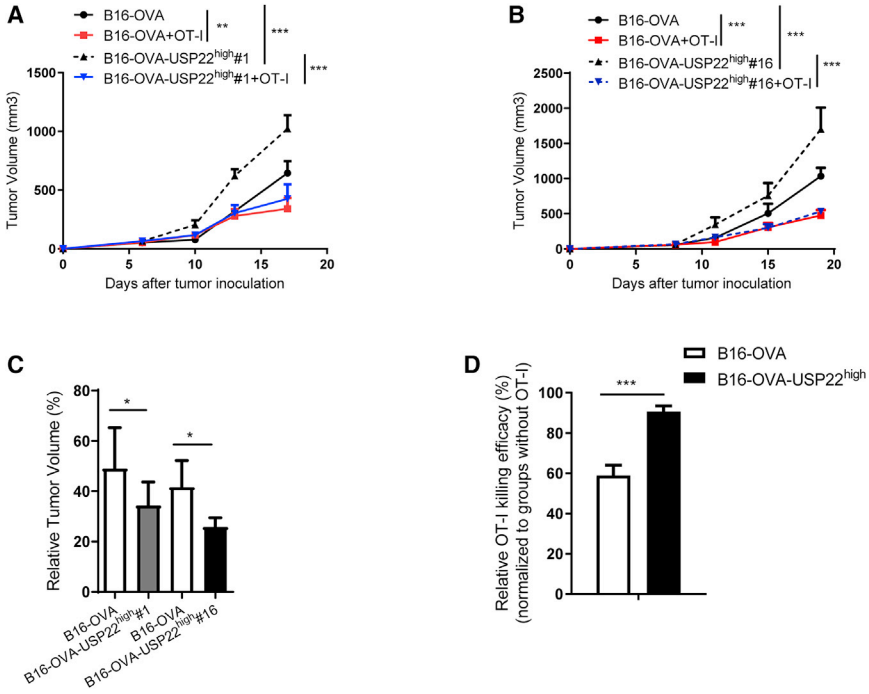

Figure 2. USP22 overexpression sensitized B16-OVA to T cell-mediated killing

(A and B) C57BL/6 mice (n = 6/group) were subcutaneously inoculated with B16-OVA, B16-OVA-USP22^{high} #1 (A), or B16-OVA-USP22^{high} #16 (B) cells followed by OT-I T cells being administered on days 7 and 10 post-tumor-inoculation. Tumor sizes were measured twice a week. Data represent means ± SEM. (C) The relative tumor volume for engrafted B16-OVA cells, B16-OVA-USP22^{high}#1 cells, and B16-OVA-USP22^{high} #16 cells on day 17 (A) and 19 (B) post-transplantation are shown. (D) B16-OVA or B16-OVA-USP22^{high} cells were cultured *in vitro* alone or with OT-I T cells for 2 days. The remaining tumor cells resistant to OT-I killing were quantified by counting trypan-blue-negative cells (left panel). The relative *in vitro* killing efficiency (ratio of remaining tumor cells in the presence of OT-I T cells compared to that in the absence of OT-I T cells is shown in the right panel. Data are shown as the mean ± SEM (A and B) or mean ± SD (C and D) . *$p < 0.05$, **$p < 0.01$, ***$p < 0.001$. Representative results of one from two (A and B) or five (D) repeated experiments are shown.

B16-OVA-USP22^{null}, and B16-OVA-JAK1^{null}USP22^{null} cells exhibited a similar resistant phenotype to OT-I T cell-mediated killing (Figure 4A). When the *Jak1* knockout was introduced into B16-OVA-USP22^{high} cells, the enhanced sensitivity to OT-I T cell-mediated killing caused by USP22 was abolished (Figure 4A).

We also compared the sensitivity of these cell lines to IFNγ treatment *in vitro*. We observed that B16-OVA-JAK1^{null}, B16-OVA-USP22^{null}, and B16-OVA-JAK1^{null} USP22^{null} cells exhibited similar resistant phenotype to IFNγ-mediated killing (Figure 4B), while *Jak1* knockout abolished the sensitivity to IFNγ in B16-OVA-USP22^{high} cells. (Figure 4B). To determine whether JAK1 could affect downstream signal activation following IFNγ stimulation, we analyzed major histocompatibility complex (MHC)-I expression by flow cytometry and the expression of representative downstream genes by qPCR (Figures 4C and 4D). Overexpression of USP22 resulted in upregulated expression of these genes, while *Jak1* knockout abolished this expression enhancement (Figures 4C and 4D). Furthermore, we observed similar positive correlation between the expression of USP22 and the components of the MHC-I complex, such as β2 m, human leukocyte antigen (HLA) -A, HLA-B, HLA-C, HLA-E, HLA-F, and HLA-G in primary human skin cutaneous melanoma patients (Figure S5). Consistent with the *in vitro* observations, B16-OVA-USP22^{high} JAK1^{null} tumor cells were resistant to treatment by the adoptive transfer of OT-I T cells, while B16-OVA-USP22^{high} tumor cells were sensitive to the same treatment (Figures 4E and S6). Taken together, these data demonstrated that the regulation of USP22 on T cell-killing sensitivity was dependent on a JAK1-related signaling pathway.

USP22 regulated the IFN signaling pathway mainly through STAT1

Since USP22 is a nuclear protein, it was possible that USP22 achieved its regulatory function by interaction with nuclear transcriptional factors. The phosphorylation, dimerization, and nuclear translocation of STATs are critical steps during IFN signal activation.[40,41] We wondered whether STATs were necessary for USP22-mediated resistance to the T cell killing. In IFNγ signaling, the mainly active STAT is STAT1 but there is weakly active STAT3.[39,42] To investigate this, we evaluated whether pharmaceutical inhibition of STAT1 and STAT3 would affect the function of USP22. We used previously determined MHC-I expression as an applicable indicator of IFN activation.[7,43] When exogenous IFNγ was present, the STAT1-specific inhibitor fludarabine dramatically reduced MHC-I expression in all three cell lines, suggesting a potent blocking effect on STAT1 activation. When exogenous IFNγ was absent, fludarabine significantly reduced the elevated expression levels of MHC-I in B16-OVA-USP22^{high} cells but had little effect on the reduction of MHC-I expression in B16-OVA-USP22^{null} cells (Figures 5A and 5C). The STAT3-specific inhibitor niclosamide was also evaluated under the same experimental conditions. Interestingly, the STAT3 inhibitor had less inhibitory effect on USP22-regulated MHC-I expression compared with STAT1 inhibitor (Figures 5B and 5C). To evaluate the influence of STAT1 and STAT3 on USP22 regulation of global IFN-related gene activation in B16-OVA-USP22^{high} cells, we used qPCR to compare the expressional levels of these genes when STAT1 or STAT3 was blocked by their respective specific inhibitors. Fludarabine treatment reduced the mRNA expression of representative genes (*ISG15*, *IRF1*, *IRF7*, *GBP3*, *BST2*, *IFI27*, and *IFI44*) (Figure 5D). However, niclosamide treatment only slightly reduced the mRNA expression of *GBP3*, *IRF1*, and *IRF7* (Figure S7). Most small molecule inhibitors exist cross activities beyond the designed target,

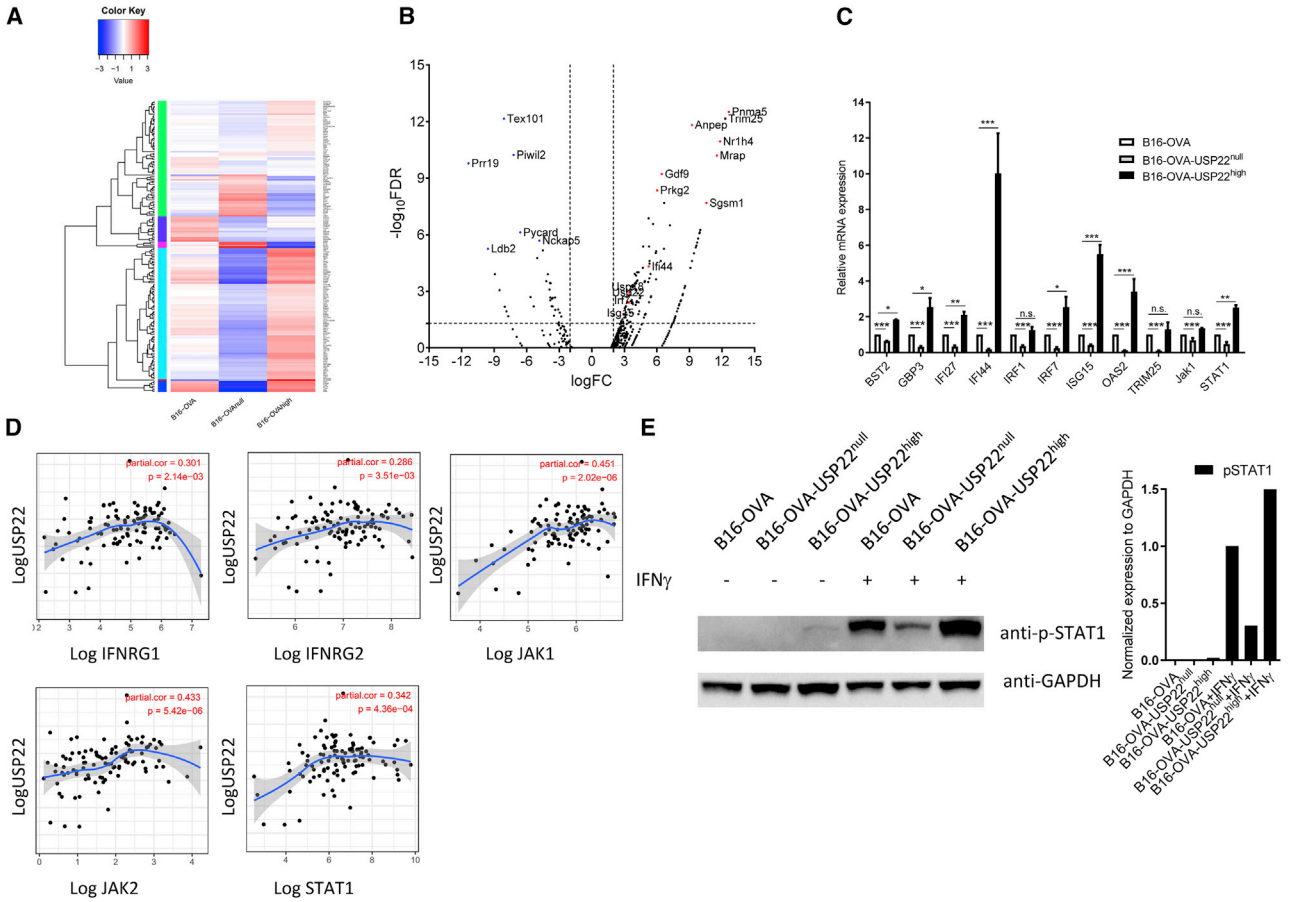

Figure 3. Global RNA sequencing revealed that USP22 activity was associated with the interferon signaling pathway

(A) Heatmap of unsupervised clustering analysis of the scaled log2-fold changes of gene expression in B16-OVA, B16-OVA-USP22^{null}, and B16-OVA-USP22^{high} cells. The cluster of heatmaps is to gather genes with similar expression patterns and display them in different color columns on the left. (B) Volcano plot of RNA-seq data of B16-OVA-USP22^{null} and B16-OVA-USP22^{high} cells. The red point (fold change > 2.0, $p < 0.05$) and blue point (fold change < −2.0, $p < 0.05$) in the plot represent statistically significant differentially expressed mRNA. (C) Quantitative PCR validation of the 11 indicated differentially expressed representative genes. (D) The correlations between USP22 and IFNγ signaling pathway molecules (IFNGR1, IFNGR2, JAK1, JAK2, and STAT1) in 103 primary human skin cutaneous melanoma patients. (E) Phosphorylation of STAT1 in B16-OVA, B16-OVA-USP22^{null}, and B16-OVA-USP22^{high} cells in the absence or presence of IFNγ. Protein expression levels were analyzed by western blot (left panel). The relative expression of p-STAT1 was quantified relative to the expression of GAPDH (right panel). Data are shown as the mean ± SD. *$p < 0.05$, **$p < 0.01$, ***$p < 0.001$. Representative results of one from two (C) or five (D) repeated experiments are shown.

and it is reported that fludarabine can competitively inhibit DNA synthesis through its metabolic active form 2F-ara-ATP.[44] To exclude the possibility of cross activity of fludarabine, we established *Stat1* and *Stat3* knockout in *USP22*-deficient or -overexpressed B16-OVA cell lines: B16-OVA-STAT1^{null}, B16-OVA-STAT3^{null}, B16-OVA-USP22^{high} STAT1^{null}, and B16-OVA-USP22^{high} STAT3^{null} cells (Figure 5E). Using previously established MHC-I expression as a readout, we compared the sensitivity of these cell lines to IFNγ treatment. When the *Stat1* knockout was introduced into B16-OVA-USP22^{high} cells, the enhanced expression of MHC-I by USP22 was abolished (Figure 5F). However, the deficiency of *Stat3* has less effect on reducing the enhanced MHC-I expression in B16-OVA-USP22^{high} cells compared with *Stat1* deficiency (Figure 5F). Similarly, we compared the sensitivity of *Stat1* and *Stat3* knockout cells to IFNγ-mediated cytotoxicity effect. Consistent with the MHC-I expression pattern, deficiency of *Stat1*, not *Stat3*, abolished USP22 overexpression-mediated super sensitivity to IFNγ in B16-OVA-USP22^{high} cells (Figure 5G). These data suggest that STAT1 was the dominant downstream transcription factor regulated by USP22.

USP22 enhanced the stability of STAT1 via deubiquitination

USP22 is a member of the USP family and is able to deubiquitinate target proteins, which may antagonize ubiquitin-mediated proteolysis.[24,45,46] It has been reported that USP22 is able to deubiquitinate SIRT1 and improves its stability.[14] We hypothesized that USP22 could regulate the activity of STAT1 through a similar mechanism. To test this hypothesis, we first compared the protein expression levels of STAT1 in B16-OVA, B16-OVA-USP22^{null}, and

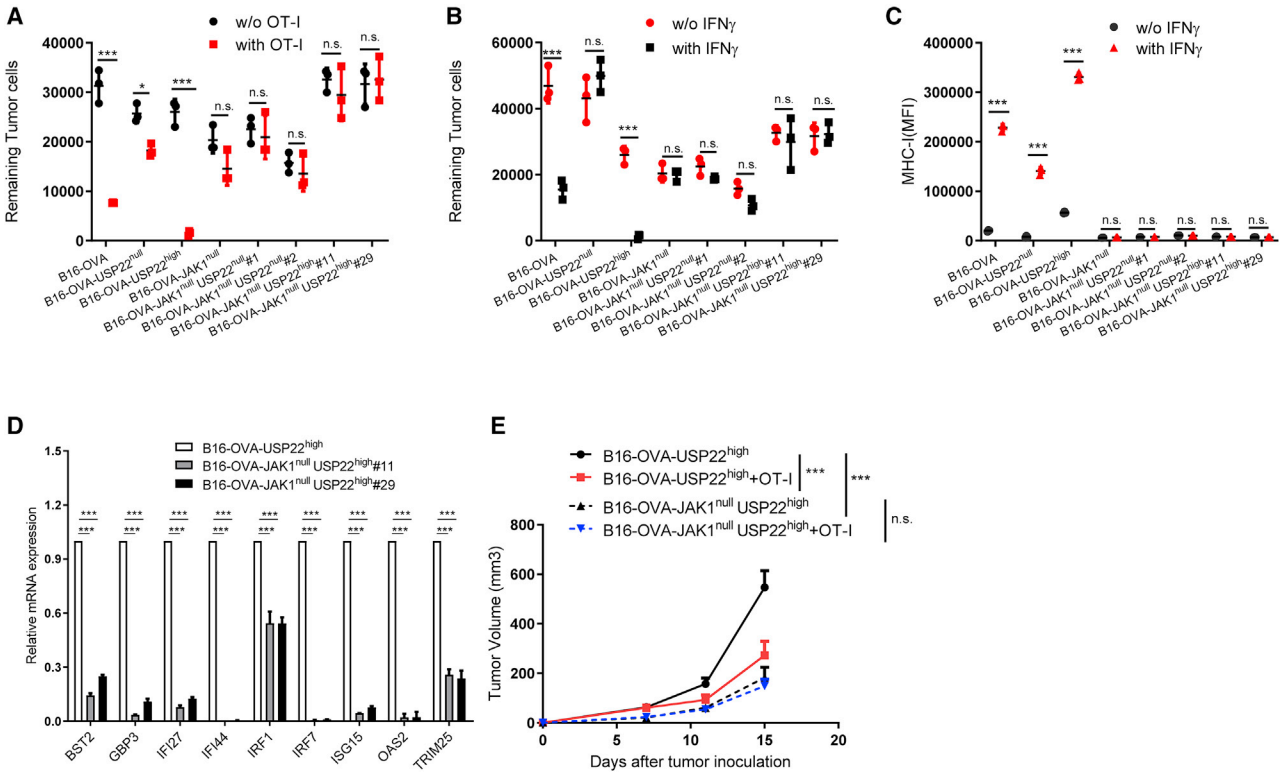

Figure 4. T cell-killing resistance mediated by *USP22* deficiency was dependent on JAK1

(A and B) The parental B16-OVA cells or derived cells indicated were co-cultured with OT-I T cells (A) or stimulated with IFNγ (B) for 3 days. The remaining tumor cells resistant to OT-I killing or IFNγ were quantified by counting trypan-blue-negative cells. (C) As in (B), the expression levels of MHC-I in the indicated cells were analyzed by flow cytometry. (D) Quantitative PCR gene expression analysis of the nine indicated representative IFN pathway-related genes in B16-OVA-USP22^{high} cells, B16-OVA-USP22^{high} JAK1^{null} #11 cells, or B16-OVA-USP22^{high} JAK1^{null} #29 cells. (E) WT C57BL/6 mice (n = 6/group) were subcutaneously inoculated with B16-OVA-USP22^{high} cells or B16-OVA-USP22^{high} JAK1^{null} #29 cells. OT-I T cells were then administered on days 7 and 10 post-engraft. Tumor sizes were measured twice a week. Data were shown as the mean ± SD (A-D) or mean ± SEM (E). *p < 0.05, ***p < 0.001. Representative results of one from three (A–C) or two (D and E) repeated experiments are shown.

B16-OVA-USP22^{high} cells. As expected, we observed a positive correlation between USP22 protein expression and STAT1 protein expression. The protein expression levels of STAT1 were highest in B16-OVA-USP22^{high} cells and lowest in B16-OVA-USP22^{null} cells (Figure 6A). This suggested the possibility of STAT1 deubiquitination by USP22. Therefore, we then evaluated whether USP22 could interact with STAT1, which would be the initial step required for deubiquitination. By immunoprecipitating STAT1 in co-immunoprecipitation (coIP) assays, we found that both ectopically expressed USP22-Flag and endogenous USP22 were able to interact with STAT1-Myc (Figure 6B). To confirm these results, we performed coIP assays in which we precipitated USP22. These assays confirmed the observed interactions between USP22-Flag and STAT1-Myc (Figure 6C).

We then tested whether USP22 was able to affect the ubiquitination of STAT1. We co-expressed USP22 and ubiquitin with STAT1 in Lenti-X 293 cells and compared the ubiquitination levels of immunoprecipitated STAT1. When USP22 was overexpressed, the ubiquitination level of STAT1 was dramatically reduced (Figure 6D). To further extend this finding, we immunoprecipitated USP22-Flag and incubated it with polyubiquitinated Myc-STAT1 in an *in vitro* deubiquitination assay. We found that USP22 significantly reduced STAT1 ubiquitination (Figure 6E) *in vitro*. We also observed similar interaction and deubiquitination of STAT3 by USP22 (Figure S8). To directly test the role of USP22 on STAT1 and STAT3 clearance, we performed cycloheximide (CHX) chase analysis. When protein synthesis was inhibited by CHX, overexpression of USP22 in B16-OVA cells reduced the rate of clearance of endogenous STAT1 and STAT3 (Figure 6F). These data suggest that USP22 could directly deubiquitinate STAT1 and STAT3 to avoid ubiquitin-mediated proteolysis and enhance the activation of IFNγ stimulation.

Human USP22 enhanced the function STAT1 through a similar deubiquitination mechanism

We have observed specific deubiquitination of STAT1 by USP22 in the mouse melanoma cell B16-OVA, which results in enhanced sensitivity to IFNγ stimulation. We wondered whether this mechanism could be applicable to human melanoma cells. To test this hypothesis, we first established *USP22*-deficient and -overexpressed human

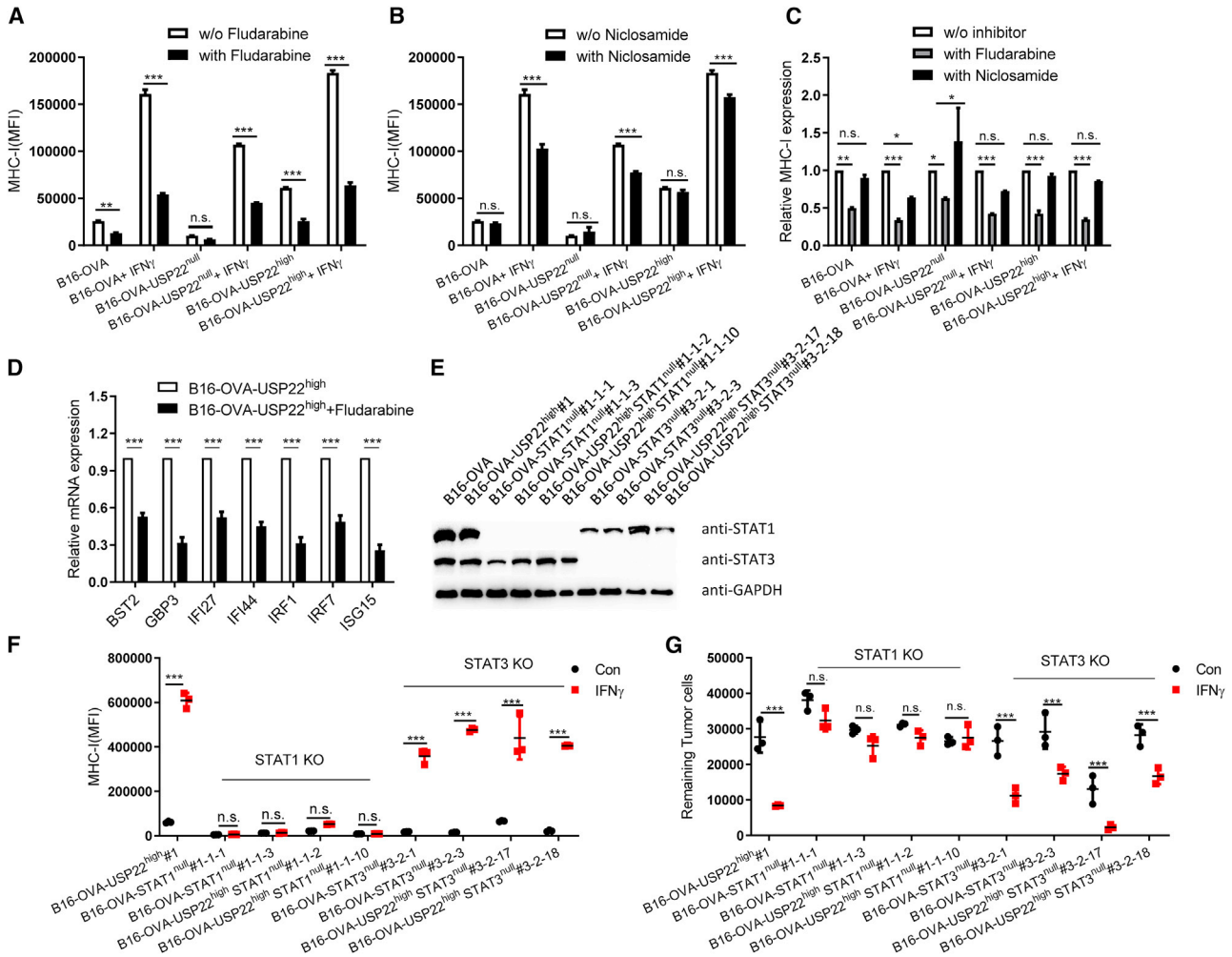

Figure 5. USP22 regulated the IFNγ signaling pathway mainly through STAT1

(A) Expression levels of MHC-I in B16-OVA-USP22^{null} or B16-OVA-USP22^{high} in the absence or presence of STAT1 inhibitor fludarabine as analyzed by flow cytometry. (B) Expression levels of MHC-I in B16-OVA-USP22^{null} or B16-OVA-USP22^{high} in the absence or presence of STAT3 inhibitor niclosamide as analyzed by flow cytometry. (C) Relative expression of MHC-I in (A) and (B). (D) Quantitative PCR gene expression analysis of the indicated representative IFN-related genes in B16-OVA-USP2^{high} cells in the presence or absence of fludarabine. (E) The expression of STAT1, STAT3, and GAPDH in indicated B16-OVA and B16-OVA-derived cells were analyzed by western blot. (F) Expression levels of MHC-I in indicated B16-OVA-derived cells in the absence or presence of IFNγ were analyzed by flow cytometry. (G) The indicated B16-OVA and B16-OVA-derived cells were stimulated with IFNγ for 3 days. The remaining tumor cells resistant to IFNγ were quantified by counting trypan-blue-negative cells. Data were shown as the mean ± SD. *p < 0.05, **p < 0.01, ***p < 0.001. Representative results of one from two repeated experiments are shown (A–G).

melanoma cell line Mel-624.[47] Interestingly, we observed a stronger positive correlation of USP22 expression and phosphorylation of STAT1 in human melanoma cell Mel-624 than mouse melanoma cell B16-OVA (Figures 3E and 7A). We then compared IFNγ-induced the HLA-β2M complex expression in USP22-knockout and -overexpression Mel-624 cell lines. The knockout of *USP22* completely abolished the HLA-β2 m complex expression in human melanoma cells (Figures 7B and S9). Furthermore, IFNγ-induced cytotoxicity was greatly enhanced in Mel-624-USP22^{high} cells, while Mel-624-USP22^{null} cells showed a resistant phenotype to IFNγ-induced cytotoxicity (Figure 7C). We wondered whether USP22 could directly interact with and impair the stability of human STAT1. As expected, we observed a positive correlation between USP22 protein expression and STAT1 protein expression in Mel-624, Mel-624-USP22^{null}, and Mel-624-USP22^{high} cells. The protein expression levels of STAT1 were the highest in Mel-624-USP22^{high} cells and lowest in Mel-624-USP22^{null} cells (Figure 7D). We then evaluated whether human USP22 could interact with STAT1 and deubiquitinate STAT1. By immunoprecipitating STAT1 in coIP assays, we found that ectopically expressed human USP22-Flag was able to interact with human STAT1-Myc (Figure 7E). We co-expressed ubiquitin with USP22 and STAT1 in the coIP assay and compared the ubiquitination levels of immunoprecipitated STAT1. When USP22 was overexpressed, the ubiquitination level of STAT1

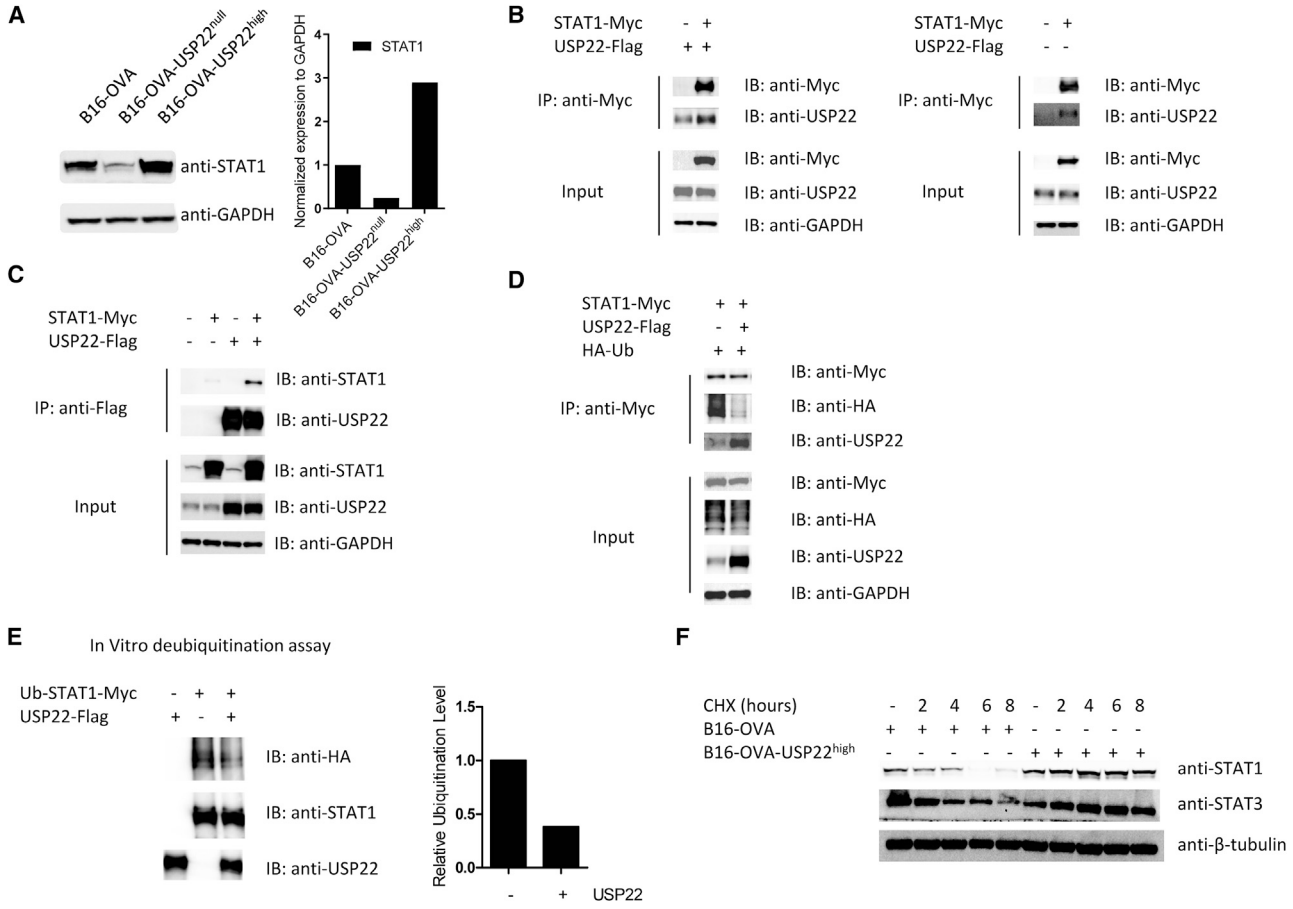

Figure 6. USP22 enhanced the stability of STAT1 through deubiquitination

(A) The expression levels of STAT1 and GAPDH in B16-OVA, B16-OVA-USP22^{null}, and B16-OVA-USP22^{high} cells were analyzed by western blot (left panel). The relative expression levels of STAT1 were quantified as the ratio of STAT1 to GAPDH (right panel). (B and C) Lenti-X 293 cells were co-transfected with the indicated STAT1-Myc and USP22-Flag plasmids (left panel) or transfected with only STAT1-Myc plasmid (right panel). Cell lysates were immunoprecipitated using an anti-Myc Ab (B) or anti-Flag Ab (C) and immunoblotted using anti-Myc, anti-STAT1, and anti-USP22 Abs. (D) Lenti-X 293 cells were co-transfected with the indicated STAT1-Myc, hemagglutinin (HA)-Ub, and USP22-Flag plasmids. Cell lysates were immunoprecipitated using an anti-Myc Ab and immunoblotted with indicated antibodies. (E) Ubiquitinated STAT1 or USP22 were immunoprecipitated from Lenti-X 293 cells co-transfected with STAT1-Myc and HA-Ub plasmids or Lenti-X 293 cells transfected with USP22. The ubiquitinated STAT1 was then incubated *in vitro* with USP22 in deubiquitination assay buffer for 20 h. The level of STAT1 ubiquitination was analyzed by western blot. (F) STAT1 and STAT3 clearance after CHX treatment (100 μg/mL) in B16-OVA and B16-OVA-USP22^{high} cells were analyzed by western blot. Representative results of one from three (A–E) repeated experiments are shown.

was dramatically reduced (Figure 7E). We also observed decreased STAT1 expression due to knockdown of USP22 in two other human melanoma cell lines: A875 and SK-MEL-1 cells (Figure S10).[48,49] Collectively, both mouse and human USP22 could directly deubiquitinate STAT1 to avoid ubiquitin-mediated proteolysis and enhance the activation of IFNγ stimulation.

DISCUSSION

Mutations widely exist in tumor cells and are driving factors of tumor development and the eventually formation of the hallmarks of cancers.[50–52] One such hallmark is the avoidance of T cell-mediated killing, which is critical for immune escape in cancers. Cancer cells use multiple mechanisms to achieve immune escape, including the upregulation of immune checkpoint ligand PD-L1 and inhibition of the antigen-presenting machinery.[53–56] Currently, immune checkpoint blockade therapies are effective in only a small portion of patients.[2,5] The mechanism of immune therapeutic resistance still remains unclear. In this study, we used pooled loss-of-function genetic screens to identify genes regulating tumor cell sensitivity to T cell-mediated killing.[37] We found that suppression of USP22 expression in tumor cells markedly reduced the cytotoxic effects mediated by T cells. In contrast, overexpression of USP22 increased the sensitivity of T cell-mediated killing. We further observed that USP22 enhanced the sensitivity of tumor cells to the key T cell effect cytokine IFNγ. Mechanically, USP22 was able to interact with STAT1 and deubiquitinate it in order to improve its stability. The improved stability of

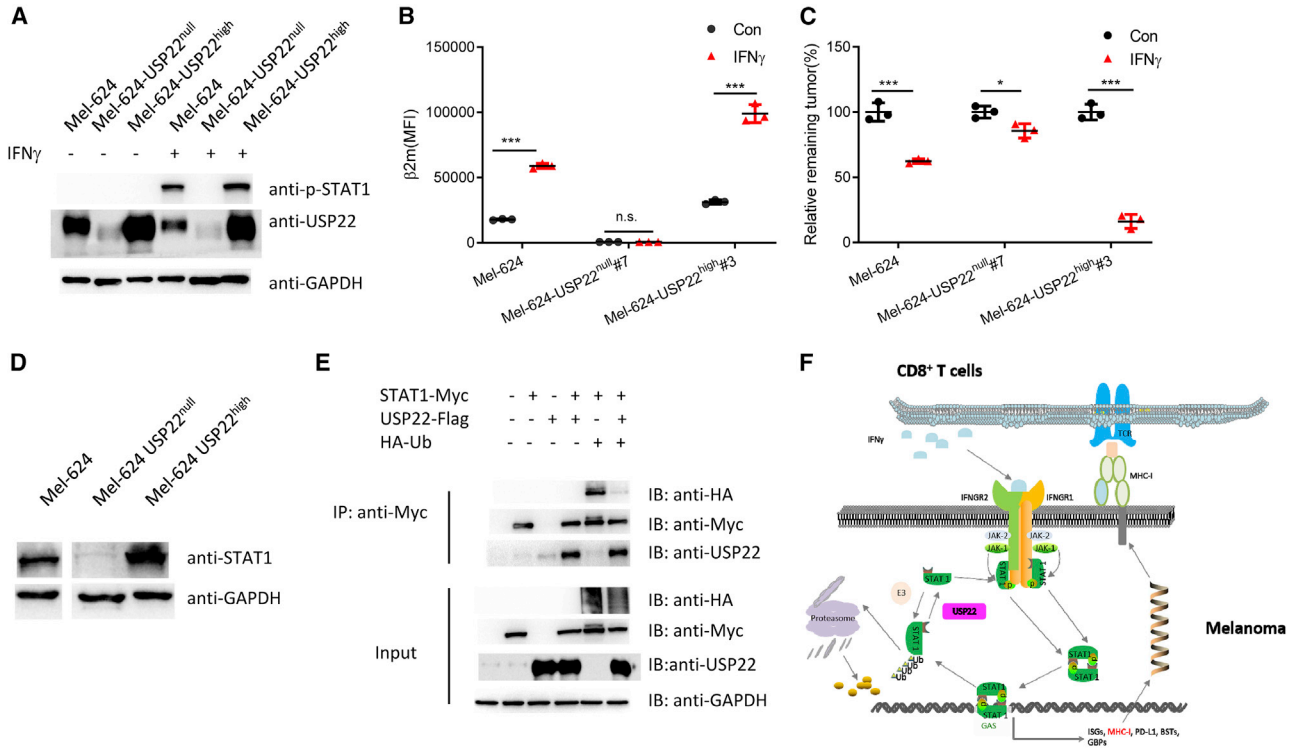

Figure 7. Human USP22 enhanced the function STAT1 through similar deubiquitination mechanism

(A) Phosphorylation of STAT1 in Mel-624, Mel-624-USP22^{null}, and Mel-624-USP22^{high} cells in the absence or presence of IFNγ. Protein expression levels were analyzed by western blot. (B) Expression levels of HLA-β2 m complex in Mel-624-USP22^{null} or Mel-624-USP22^{high} with the absence or presence of IFNγ were analyzed by flow cytometry. (C) The parental Mel-624 cells or derived cells were stimulated with IFNγ for 3 days. The remaining tumor cells resistant to IFNγ were quantified by counting trypan-blue-negative cells. (D) The expression levels of STAT1 and GAPDH in Mel-624, Mel-624-USP22^{null}, and Mel-624-USP22^{high} cells were analyzed by western blot. (E) Lenti-X 293 cells were co-transfected with the indicated human STAT1-Myc, HA-Ub, and human USP22-Flag plasmids. Cell lysates were immunoprecipitated using an anti-Myc Ab and immunoblotted with indicated antibodies. (F) Proposed model of how USP22 regulates IFNGR/JAK1/STAT1 signaling pathways through deubiquitinating STAT1 in melanoma cells. T cell-released IFNγ transduces its activation signals through binding with receptors IFNGR1 and IFNGR2 on melanoma cells, which leads to the recruitment and activation of JAK1 and JAK2. Upon phosphorylation by JAK1, pSTAT1 homodimers then translocate to the nucleus, where they bind to specific promoter elements and modulate the transcription of IFN-regulated genes including *ISGs*, *GBPs*, *MHC-I*, and *PD-L1*. Upregulation of MHC-I complex sensitizes melanoma cells to T cell-mediated killing. USP22 can deubiquitinate STAT-1, which decreases proteasome-mediated degradation of STAT1. By this mechanism, USP22 enhances the sensitivity of the JAK-STAT signaling pathway. When USP22 is deficient in melanoma cells, more STAT1 is degraded, IFNγ-mediated signal activation is compromised, and melanoma cells are resistant to T cell-mediated killing. Data are shown as the mean ± SD. *$p < 0.05$, ***$p < 0.001$. Representative results of one from three (A–E) repeated experiments are shown.

STAT1 increased the sensitivity of the IFNγ-JAK1-STAT1 signaling pathway (Figure 7F). Our study revealed an undiscovered and essential role of USP22 in tumor cell immune escape from T cells by modulating the IFNγ-JAK1-STAT1 signaling pathway in target tumor cells.

Previous research regarding USP22 has focused on its tumor-promoting capabilities through the deubiquitination of target proteins. For instance, USP22 is able to antagonize p53 transcriptional activation by stabilizing SIRT1 and reducing apoptosis.[15] USP22 can also promote cell proliferation and tumorigenesis in colon cancer by deubiquitinating CCNB1[23] and promote tumorigenesis in glioblastoma by deubiquitinating KDM1A.[24] USP22, as a subunit of the SAGA complex, is able to deubiquitinate histone H2B and regulate Myc-activated transformation.[12] It is possible that USP22 regulates the stability of STAT1 through the SAGA complex. To test this possibility, we established two SAGA complex component (general control transcription factor [GCN] 5 and TATA-box binding protein associated factor [TAF] 9) knockout/knockdown B16-OVA melanoma cells and evaluated the JAK1-STAT1 pathway signature in these cells. As opposed to B16-OVA-USP22^{null} cells, we observed increased expression of STAT1 in these cells (Figure S11). It suggested that USP22-mediated STAT1 stabilization is not dependent on SAGA complex. In addition to these intrinsic tumor mechanisms, we also showed that USP22 was able to regulate the JAK1-STAT1 signaling pathway, which contributed to the immune escape from T cells. This is consistent with recent studies that revealed an important role for the IFN-JAK1-STAT1 signal in regulating immune therapy resistance. It has been reported that *Jak1/2* mutations are related to immunotherapy resistance,[7,57] and studies have described multiple important regulators of the IFN-JAK1-STAT1 signaling pathway, including PTPN2,

APLNR, and LILRB4.[6,58,59] Our current study identifies USP22 as a positive regulator of the IFN-JAK1-STAT1 pathway through the deubiquitination of STAT1. It will be interesting to investigate whether other deubiquitinating enzymes are able to modify the IFN-JAK1-STAT1 signaling pathway, which may provide potential therapeutic targets for enhancing the efficacy of T cell-based immunotherapy. While we were preparing our manuscript, Huang et al.[29] and Cai et al.[60] reported that USP22 is able to directly deubiquitinate PD-L1 and KPNA2 to improve their stability, both of which are related to IFN pathway. Based on our observation, USP22 can directly deubiquitinate STAT1, which suggests that USP22 can regulate the IFN pathway at multiple levels.

Our data also indicate that USP22 deficiency could decrease the expression of MHC-I (Figures 4C, 7B, and S9). Since MHC-I-peptide complex is the first signal for T cell activation and important inhibitory ligand for natural killer (NK) cells, *USP22* deficiency will affect the anti-tumor immunity through both T cell and NK cells. In *USP22*-deficient tumor cells, the expression of MHC-I is low, which may lead to activation of NK cells. Indeed, we observed increased activation of NK cells in B16-OVA-USP22^{null} tumor microenvironment than in parental B16-OVA. In addition, NK92 cells produced more IFNγ when co-cultured with Mel-624-USP22^{null} than parental M624 cells (Figure S12). These data highlighted the complicated role of USP22 in regulating anti-tumor immune responses. It will be interesting to investigate the USP22-mediated dynamic impact on NK cells and T cell in different tumor development stages in the future.

Recent studies have also shown that the T cell effect cytokine IFNγ exerts an anti-tumor effect by causing endothelial cells of blood vessels to reduce angiogenesis in the tumor stroma.[61] Given our finding that USP22 regulates the IFN signaling pathway in tumor cells, it is possible that USP22 stabilizes STAT1 to augment the IFNγ response to angiogenesis in endothelial cells and ultimately enhance the anti-tumor activity mediated by T cells. It will be interesting to investigate USP22 expression and function on tumor blood vessels and stromal cells in future studies. Type II and type I IFN pathways share STAT1 as a common transcriptional factor. Therefore, USP22 could theoretically also regulate the type I IFN signaling pathway. In addition to tumor cells and stroma cells, the type I IFN pathway has been shown to play a critical regulatory role in multiple types of immune cells. Type I IFN could activate dendritic cell (DC) and macrophage to promote antigen presentation.[62,63] Type I IFN is able to directly activate both NK and T cells to enhance their cytotoxic abilities.[62] Further studies on the role of USP22 in these immune cells will provide a deeper, more comprehensive understanding of USP22 in the tumor microenvironment.

Functional genomic approaches utilizing whole-genome editing strategies have been used to identify genes required by tumor cells for establishing the cancer hallmarks of growth, metastasis, drug resistance, and immune escape.[6,64–69] Our study also took advantage of this approach to investigate the interaction of tumor cells with tumor-specific T cells. Our studies revealed that the tumor stem feature-related gene USP22 modified the sensitivity of tumor cells to T cell killing by regulating the IFN-JAK1-STAT1 signaling pathway. Our results defined a dual regulatory role of USP22 for both the tumor itself and the surrounding immune system. The careful evaluation of similar regulatory genes in both tumor cells and immune cells may lead to the development of potent anti-cancer drugs. We believe that this screening approach can be broadly applied to the systematic identification of novel mechanisms involved in immune escape and will be beneficial in the development of new drugs to circumvent these escape mechanisms.

MATERIALS AND METHODS

Mice

OT-I-Tg mice were purchased from The Jackson Laboratory (Bar Harbor, ME, USA). 6- to 9-week-old female C57BL/6 mice were purchased from Beijing Charles River Laboratory Animal Technology (Beijing, China). All mice were maintained under specific pathogen-free conditions. Animal care and use were carried out in accordance with institutional and National Institutes of Health protocols and guidelines, and all studies were approved by the Animal Care and Use Committee of Shanghai Jiao Tong University.

Cell lines and reagents

Lenti-X 293 cells were purchased from Clontech. B16-OVA cells were provided by Hans Schreiber (University of Chicago). Mel-624 cells were established by the Surgery Branch, NCI, as previously described.[70] A875 and SK-MEL-1 cells were purchased from Procell Life Science &Technology. NK92 cells were purchased from the American Type Culture Collection. B16-OVA-USP22^{high} cells were generated by infection of the cells with lentivirus expressing mouse USP22. B16-OVA-USP22^{null}, B16-OVA-JAK1^{null}, B16-OVA-JAK1^{null} USP22^{null}, B16-OVA-STAT1^{null}, B16-OVA-STAT3^{null}, B16-OVA-USP22^{high} STAT1^{null}, and B16-OVA-USP22^{high} STAT3^{null} cells were generated by infection of parental B16-OVA or B16-OVA-USP22^{high} cells with lentivirus expressing Cas9 and sgRNA specific for *USP22*, *Jak1*, *Stat1*, or *Stat3*. All stable cell lines were cloned by limited dilution. Mel-624-derived tumor cells were generated similarly to B16-OVA-derived cells. All cells were cultured at 37°C under 5% CO_2. Lenti-X 293, B16-OVA cells, and their derivatives were cultured in Dulbecco's modified Eagle's medium (DMEM). A875 and SK-MEL-1 cells were cultured in MEMα medium. NK92 and OT-I T cells from OT-I-Tg mice were cultured in RPMI 1640 medium. All culture media were supplemented with 10% heat-inactivated fetal bovine serum (Gibco, Grand Island, NY, USA), 2 mmol/L L-glutamine, 100 U/mL penicillin, and 100 μg/mL streptomycin. The sgRNA and short hairpin RNA (shRNA) sequences are listed in Table S3.

Screening of genes related to T cell resistance

The B16-OVA cell line was infected with the lentiviral mouse CRISPR KO (GeCKO) v2.0 pooled library.[37] Equal number of pooled GeCKO-B16-OVA cells and OT-I T cells were then subcutaneously injected into the right flank of mice . One month later, the mice were sacrificed, the tumors removed and digested, and the dissociated tumor

cells cultured. Genomic DNA was isolated from the cultured cells using an E.Z.N.A. tissue DNA kit I (Omega Bio-tek). The integrated sgRNA cassette was PCR amplified and sequenced by Genewiz (Suzhou, China) using next-generation sequencing (NGS).

Cell proliferation analysis *in vitro*

Cell viability was measured using the Cell Counting Kit-8 (CCK-8) assay. Cells were seeded into 96-well plates at a density of 3×10^3 cells/well and placed in an incubator until the cells grew to confluence. Each cell has four replicates in each condition. Subsequently, 10 μL of CCK-8 solution was added at different time points (24, 48, and 72 h), and the samples were incubated at 37°C for 90 min. The absorbance value of each well was measured at 450 nm using a microplate reader. We also counted the number of tumor cells at different conditions 72 h later to explore the cell proliferation.

Tumor growth and treatments

Approximately 5×10^5 cells of B16-OVA, B16-OVA-USP22^{null} #1–8, B16-OVA-USP22^{null} #1–9, B16-OVA-USP22^{high} #1, B16-OVA-USP22 ^{high} #16, or other indicated derivatives were subcutaneously injected on the right flank of C57BL/6 mice. Splenocytes from OT-I-Tg mice were intratumorally injected when tumor was palpable with the volumes between 40 mm^3 and 60 mm^3. Tumor volumes were measured along three orthogonal axes (a, b, and c) and tumor volumes calculated using the equation $(a \times b \times c)/2$.

Western blotting and coIP

B16-OVA cells and their derivatives were untreated or treated with IFNγ for 30 min and lysed in 1× radioimmunoprecipitation assay (RIPA) lysis buffer containing 1× protease inhibitor cocktail, 1 mM phenylmethylsulfonyl fluoride (PMSF), and 1 mM sodium orthovanadate. In CHX-chase analysis, B16-OVA and B16-OVA-USP22^{high} cells were treated with 100 μg/mL of CHX for 0, 2, 4, or 8 h, and STAT1 and STAT3 expression in total cell lysate was analyzed by western blotting. Western blotting was performed as previously described.[46]

Lenti-X 293 cells in 6-well plates were transfected with the indicated plasmids. At 60 h post-transfection, cells were lysed with 500 μL of immunoprecipitation buffer (50 mM HEPES [pH 7.3]; 50 mM NaCl; 1% Triton X-100; 10% glycerol; 5 mM EDTA) supplemented with 1× protease inhibitor cocktail, 1 mM PMSF, and 1 mM sodium orthovanadate. For immunoprecipitation, 1 μg of the indicated antibody was incubated with cell lysates for 4 h at 4°C. Then, 10 μL of protein A-diamond agarose beads (Bestchrom) was added to the lysates and incubated overnight on the roller. The protein A beads were washed three times with immunoprecipitation buffer and boiled in 2× sodium dodecyl sulfate (SDS) loading buffer. Western blotting was performed as previously described.[71] The antibodies used for immunoprecipitation and other reagents are listed in Table S4.

Analysis of gene expression correlation in human primary melanoma patients

The correlation between USP22 and key molecules (IFNGR1, IFNGR2, JAK1, JAK2, and STAT1) of the IFN signaling pathway in primary human skin cutaneous melanoma patients was analyzed by Tumor Immune Estimation Resource (TIMER) (https://cistrome.shinyapps.io/timer/).

qPCR

Total RNA was extracted using an E.Z.N.A. Total RNA Kit I (Omega Bio-Tek). The RNA was reverse transcribed using ReverTra Ace reverse transcriptase (Toyobo) and gene expression of the specified genes quantified using KOD SYBR qPCR mix (Toyobo) according to manufacturer's instructions. The PCR primer sequences were listed in Table S5.

Flow cytometric analysis

Single-cell suspensions of cells were incubated with anti-CD16/32 (anti-FcgIII/II receptor, clone 2.4G2) for 10 min and then stained with conjugated Abs indicated. All fluorescently labeled monoclonal antibodies (mAbs) were purchased from Biolegend or eBioscience. Samples were analyzed on a Cytoflex flow cytometer (Beckman Coulter) and the data analyzed using FlowJo software V10 (TreeStar).

In vitro deubiquitination assays

Lenti-X 293 cells were co-transfected with HA-ubiquitin and Myc-STAT1 plasmids and Myc-tagged ubiquitinated STAT1 was immunoprecipitated using an anti-Myc antibody. In parallel experiments, Flag-USP22 was immunoprecipitated from USP22-transfected Lenti-X 293 cells using anti-Flag antibody. For *in vitro* deubiquitination assays, ubiquitinated Myc-STAT1 was incubated with USP22-Flag in deubiquitination reaction buffer (50 mM HEPES [pH 7.5]; 100 mM NaCl; 5% glycerol; 5 mM $MgCl_2$; 1 mM ATP; and 1 mM DTT) at 30°C for 20 h as previously described.[72] The reaction mixtures were denatured in SDS loading buffer, separated by SDS-polyacrylamide gel electrophoresis (PAGE), and analyzed by western blot.[71–73]

Statistical analysis

Data are expressed as means ± standard error of the mean (SEM) or standard deviation (SD). The data were compared using two-tailed unpaired Student's t test compared with two groups. When more than two groups were analyzed, one-way ANOVA Tukey's multiple comparison test was performed. p values were calculated using GraphPad Prism software (v5). Values were considered statistically different when $^*p < 0.05$, $^{**}p < 0.01$, $^{***}p < 0.001$.

SUPPLEMENTAL INFORMATION

Supplemental Information can be found online at https://doi.org/10.1016/j.ymthe.2021.02.018.

ACKNOWLEDGMENTS

We thank Dr. Jie Zhao for comments and editing of this paper. X.Y. was supported by the National Natural Science Foundation of China (81971467 and 81671643), the National Key Research and Development Program of China (2016YFC1303400), and Shanghai Jiao Tong University Scientific and Technological Innovation Funds. P.H. was supported by the National Natural Science Foundation of China (81901689).

AUTHOR CONTRIBUTIONS

X.Y. designed the overall project. M.L., Y.X., J.L., H.L., X.Q., F.L., P.H., Y.G., and X.Y. performed the experiments. M.L., Y.X., and X.Y. analyzed the results and wrote the manuscript.

DECLARATION OF INTERESTS

The authors declare no competing interests.

REFERENCES

1. Chen, D.S., and Mellman, I. (2017). Elements of cancer immunity and the cancer-immune set point. Nature *541*, 321–330.
2. Hodi, F.S., O'Day, S.J., McDermott, D.F., Weber, R.W., Sosman, J.A., Haanen, J.B., Gonzalez, R., Robert, C., Schadendorf, D., Hassel, J.C., et al. (2010). Improved survival with ipilimumab in patients with metastatic melanoma. N. Engl. J. Med. *363*, 711–723.
3. Motzer, R.J., Tannir, N.M., McDermott, D.F., Arén Frontera, O., Melichar, B., Choueiri, T.K., Plimack, E.R., Barthélémy, P., Porta, C., George, S., et al.; CheckMate 214 Investigators (2018). Nivolumab plus Ipilimumab versus Sunitinib in Advanced Renal-Cell Carcinoma. N. Engl. J. Med. *378*, 1277–1290.
4. Hellmann, M.D., Ciuleanu, T.E., Pluzanski, A., Lee, J.S., Otterson, G.A., Audigier-Valette, C., Minenza, E., Linardou, H., Burgers, S., Salman, P., et al. (2018). Nivolumab plus Ipilimumab in Lung Cancer with a High Tumor Mutational Burden. N. Engl. J. Med. *378*, 2093–2104.
5. Page, D.B., Postow, M.A., Callahan, M.K., Allison, J.P., and Wolchok, J.D. (2014). Immune modulation in cancer with antibodies. Annu. Rev. Med. *65*, 185–202.
6. Manguso, R.T., Pope, H.W., Zimmer, M.D., Brown, F.D., Yates, K.B., Miller, B.C., Collins, N.B., Bi, K., LaFleur, M.W., Juneja, V.R., et al. (2017). In vivo CRISPR screening identifies Ptpn2 as a cancer immunotherapy target. Nature *547*, 413–418.
7. Han, P., Dai, Q., Fan, L., Lin, H., Zhang, X., Li, F., and Yang, X. (2019). Genome-Wide CRISPR Screening Identifies JAK1 Deficiency as a Mechanism of T-Cell Resistance. Front. Immunol. *10*, 251.
8. Kleppe, M., Soulier, J., Asnafi, V., Mentens, N., Hornakova, T., Knoops, L., Constantinescu, S., Sigaux, F., Meijerink, J.P., Vandenberghe, P., et al. (2011). PTPN2 negatively regulates oncogenic JAK1 in T-cell acute lymphoblastic leukemia. Blood *117*, 7090–7098.
9. Kleppe, M., Lahortiga, I., El Chaar, T., De Keersmaecker, K., Mentens, N., Graux, C., Van Roosbroeck, K., Ferrando, A.A., Langerak, A.W., Meijerink, J.P., et al. (2010). Deletion of the protein tyrosine phosphatase gene PTPN2 in T-cell acute lymphoblastic leukemia. Nat. Genet. *42*, 530–535.
10. Nijman, S.M., Luna-Vargas, M.P., Velds, A., Brummelkamp, T.R., Dirac, A.M., Sixma, T.K., and Bernards, R. (2005). A genomic and functional inventory of deubiquitinating enzymes. Cell *123*, 773–786.
11. Cole, A.J., Clifton-Bligh, R., and Marsh, D.J. (2015). Histone H2B monoubiquitination: roles to play in human malignancy. Endocr. Relat. Cancer *22*, T19–T33.
12. Zhang, X.Y., Varthi, M., Sykes, S.M., Phillips, C., Warzecha, C., Zhu, W., Wyce, A., Thorne, A.W., Berger, S.L., and McMahon, S.B. (2008). The putative cancer stem cell marker USP22 is a subunit of the human SAGA complex required for activated transcription and cell-cycle progression. Mol. Cell *29*, 102–111.
13. Armour, S.M., Bennett, E.J., Braun, C.R., Zhang, X.Y., McMahon, S.B., Gygi, S.P., Harper, J.W., and Sinclair, D.A. (2013). A high-confidence interaction map identifies SIRT1 as a mediator of acetylation of USP22 and the SAGA coactivator complex. Mol. Cell. Biol. *33*, 1487–1502.
14. Ao, N., Liu, Y., Feng, H., Bian, X., Li, Z., Gu, B., Zhao, X., and Liu, Y. (2014). Ubiquitin-specific peptidase USP22 negatively regulates the STAT signaling pathway by deubiquitinating SIRT1. Cell. Physiol. Biochem *33*, 1863–1875.
15. Lin, Z., Yang, H., Kong, Q., Li, J., Lee, S.M., Gao, B., Dong, H., Wei, J., Song, J., Zhang, D.D., and Fang, D. (2012). USP22 antagonizes p53 transcriptional activation by deubiquitinating Sirt1 to suppress cell apoptosis and is required for mouse embryonic development. Mol. Cell *46*, 484–494.
16. Kim, T.H., Yang, Y.M., Han, C.Y., Koo, J.H., Oh, H., Kim, S.S., You, B.H., Choi, Y.H., Park, T.S., Lee, C.H., et al. (2018). Gα12 ablation exacerbates liver steatosis and obesity by suppressing USP22/SIRT1-regulated mitochondrial respiration. J. Clin. Invest. *128*, 5587–5602.
17. Li, L., Osdal, T., Ho, Y., Chun, S., McDonald, T., Agarwal, P., Lin, A., Chu, S., Qi, J., Li, L., et al. (2014). SIRT1 activation by a c-MYC oncogenic network promotes the maintenance and drug resistance of human FLT3-ITD acute myeloid leukemia stem cells. Cell Stem Cell *15*, 431–446.
18. Glinsky, G.V., Berezovska, O., and Glinskii, A.B. (2005). Microarray analysis identifies a death-from-cancer signature predicting therapy failure in patients with multiple types of cancer. J. Clin. Invest. *115*, 1503–1521.
19. Glinsky, G.V. (2006). Genomic models of metastatic cancer: functional analysis of death-from-cancer signature genes reveals aneuploid, anoikis-resistant, metastasis-enabling phenotype with altered cell cycle control and activated Polycomb Group (PcG) protein chromatin silencing pathway. Cell Cycle *5*, 1208–1216.
20. Yang, X., Zang, H., Luo, Y., Wu, J., Fang, Z., Zhu, W., and Li, Y. (2018). High expression of USP22 predicts poor prognosis and advanced clinicopathological features in solid tumors: a meta-analysis. OncoTargets Ther. *11*, 3035–3046.
21. Tang, B., Tang, F., Li, B., Yuan, S., Xu, Q., Tomlinson, S., Jin, J., Hu, W., and He, S. (2015). High USP22 expression indicates poor prognosis in hepatocellular carcinoma. Oncotarget *6*, 12654–12667.
22. He, Y., Jin, Y.J., Zhang, Y.H., Meng, H.X., Zhao, B.S., Jiang, Y., Zhu, J.W., Liang, G.Y., Kong, D., and Jin, X.M. (2015). Ubiquitin-specific peptidase 22 overexpression may promote cancer progression and poor prognosis in human gastric carcinoma. Transl. Res. *165*, 407–416.
23. Lin, Z., Tan, C., Qiu, Q., Kong, S., Yang, H., Zhao, F., Liu, Z., Li, J., Kong, Q., Gao, B., et al. (2015). Ubiquitin-specific protease 22 is a deubiquitinase of CCNB1. Cell Discov. *1*, 15028.
24. Zhou, A., Lin, K., Zhang, S., Chen, Y., Zhang, N., Xue, J., Wang, Z., Aldape, K.D., Xie, K., Woodgett, J.R., and Huang, S. (2016). Nuclear GSK3β promotes tumorigenesis by phosphorylating KDM1A and inducing its deubiquitylation by USP22. Nat. Cell Biol. *18*, 954–966.
25. Liang, J.X., Ning, Z., Gao, W., Ling, J., Wang, A.M., Luo, H.F., Liang, Y., Yan, Q., and Wang, Z.Y. (2014). Ubiquitin-specific protease 22-induced autophagy is correlated with poor prognosis of pancreatic cancer. Oncol. Rep. *32*, 2726–2734.
26. Ning, Z., Wang, A., Liang, J., Xie, Y., Liu, J., Feng, L., Yan, Q., and Wang, Z. (2014). USP22 promotes the G1/S phase transition by upregulating FoxM1 expression via β-catenin nuclear localization and is associated with poor prognosis in stage II pancreatic ductal adenocarcinoma. Int. J. Oncol. *45*, 1594–1608.
27. Zhang, Y., Yao, L., Zhang, X., Ji, H., Wang, L., Sun, S., and Pang, D. (2011). Elevated expression of USP22 in correlation with poor prognosis in patients with invasive breast cancer. J. Cancer Res. Clin. Oncol. *137*, 1245–1253.
28. Ling, S., Shan, Q., Zhan, Q., Ye, Q., Liu, P., Xu, S., He, X., Ma, J., Xiang, J., Jiang, G., et al. (2020). USP22 promotes hypoxia-induced hepatocellular carcinoma stemness by a HIF1α/USP22 positive feedback loop upon TP53 inactivation. Gut *69*, 1322–1334.
29. Huang, X., Zhang, Q., Lou, Y., Wang, J., Zhao, X., Wang, L., Zhang, X., Li, S., Zhao, Y., Chen, Q., et al. (2019). USP22 Deubiquitinates CD274 to Suppress Anticancer Immunity. Cancer Immunol. Res. *7*, 1580–1590.
30. Ikeda, H., Old, L.J., and Schreiber, R.D. (2002). The roles of IFN gamma in protection against tumor development and cancer immunoediting. Cytokine Growth Factor Rev. *13*, 95–109.
31. Gao, J., Shi, L.Z., Zhao, H., Chen, J., Xiong, L., He, Q., Chen, T., Roszik, J., Bernatchez, C., Woodman, S.E., et al. (2016). Loss of IFN-γ Pathway Genes in Tumor Cells as a Mechanism of Resistance to Anti-CTLA-4 Therapy. Cell *167*, 397–404.e9.
32. Lyngaa, R., Pedersen, N.W., Schrama, D., Thrue, C.A., Ibrani, D., Met, O., Straten, P.T., Nghiem, P., Becker, J.C., and Hadrup, S.R. (2014). T-cell responses to oncogenic merkel cell polyomavirus proteins distinguish patients with merkel cell carcinoma from healthy donors. Clin. Cancer Res *20*, 1768–1778.
33. Martinez-Lostao, L., Anel, A., and Pardo, J. (2015). How Do Cytotoxic Lymphocytes Kill Cancer Cells? Clin. Cancer Res *21*, 5047–5056.
34. Massagué, J., and Obenauf, A.C. (2016). Metastatic colonization by circulating tumour cells. Nature *529*, 298–306.

35. Liu, C., Chikina, M., Deshpande, R., Menk, A.V., Wang, T., Tabib, T., Brunazzi, E.A., Vignali, K.M., Sun, M., Stolz, D.B., et al. (2019). Treg Cells Promote the SREBP1-Dependent Metabolic Fitness of Tumor-Promoting Macrophages via Repression of $CD8^+$ T Cell-Derived Interferon-γ. Immunity *51*, 381–397.e6.

36. Zhang, X., Cheng, C., Hou, J., Qi, X., Wang, X., Han, P., and Yang, X. (2019). Distinct contribution of PD-L1 suppression by spatial expression of PD-L1 on tumor and non-tumor cells. Cell. Mol. Immunol. *16*, 392–400.

37. Sanjana, N.E., Shalem, O., and Zhang, F. (2014). Improved vectors and genome-wide libraries for CRISPR screening. Nat. Methods *11*, 783–784.

38. Boissonnas, A., Licata, F., Poupel, L., Jacquelin, S., Fetler, L., Krumeich, S., Théry, C., Amigorena, S., and Combadière, C. (2013). CD8+ tumor-infiltrating T cells are trapped in the tumor-dendritic cell network. Neoplasia *15*, 85–94.

39. Qing, Y., and Stark, G.R. (2004). Alternative activation of STAT1 and STAT3 in response to interferon-gamma. J. Biol. Chem. *279*, 41679–41685.

40. Schneider, W.M., Chevillotte, M.D., and Rice, C.M. (2014). Interferon-stimulated genes: a complex web of host defenses. Annu. Rev. Immunol. *32*, 513–545.

41. Ivashkiv, L.B., and Donlin, L.T. (2014). Regulation of type I interferon responses. Nat. Rev. Immunol. *14*, 36–49.

42. Ivashkiv, L.B. (2018). IFNγ: signalling, epigenetics and roles in immunity, metabolism, disease and cancer immunotherapy. Nat. Rev. Immunol. *18*, 545–558.

43. Matte-Martone, C., Liu, J., Zhou, M., Chikina, M., Green, D.R., Harty, J.T., and Shlomchik, W.D. (2017). Differential requirements for myeloid leukemia IFN-γ conditioning determine graft-versus-leukemia resistance and sensitivity. J. Clin. Invest. *127*, 2765–2776.

44. Plunkett, W., Huang, P., and Gandhi, V. (1990). Metabolism and action of fludarabine phosphate. Semin. Oncol. *17* (*Suppl 8*), 3–17.

45. Zou, Q., Jin, J., Hu, H., Li, H.S., Romano, S., Xiao, Y., Nakaya, M., Zhou, X., Cheng, X., Yang, P., et al. (2014). USP15 stabilizes MDM2 to mediate cancer-cell survival and inhibit antitumor T cell responses. Nat. Immunol. *15*, 562–570.

46. Peng, H., Yang, F., Hu, Q., Sun, J., Peng, C., Zhao, Y., and Huang, C. (2020). The ubiquitin-specific protease USP8 directly deubiquitinates SQSTM1/p62 to suppress its autophagic activity. Autophagy *16*, 698–708.

47. Kaler, P., Owusu, B.Y., Augenlicht, L., and Klampfer, L. (2014). The Role of STAT1 for Crosstalk between Fibroblasts and Colon Cancer Cells. Front. Oncol. *4*, 88.

48. Tilly, B.C., Tertoolen, L.G., Remorie, R., Ladoux, A., Verlaan, I., de Laat, S.W., and Moolenaar, W.H. (1990). Histamine as a growth factor and chemoattractant for human carcinoma and melanoma cells: action through Ca2(+)-mobilizing H1 receptors. J. Cell Biol. *110*, 1211–1215.

49. Kunter, U., Buer, J., Probst, M., Duensing, S., Dallmann, I., Grosse, J., Kirchner, H., Schluepen, E.M., Volkenandt, M., Ganser, A., and Atzpodien, J. (1996). Peripheral blood tyrosinase messenger RNA detection and survival in malignant melanoma. J. Natl. Cancer Inst. *88*, 590–594.

50. Balmain, A. (2020). The critical roles of somatic mutations and environmental tumor-promoting agents in cancer risk. Nat. Genet. *52*, 1139–1143.

51. Brégeon, D., and Doetsch, P.W. (2011). Transcriptional mutagenesis: causes and involvement in tumour development. Nat. Rev. Cancer *11*, 218–227.

52. Leroi, A.M., Koufopanou, V., and Burt, A. (2003). Cancer selection. Nat. Rev. Cancer *3*, 226–231.

53. Su, S., Zhao, J., Xing, Y., Zhang, X., Liu, J., Ouyang, Q., Chen, J., Su, F., Liu, Q., and Song, E. (2018). Immune Checkpoint Inhibition Overcomes ADCP-Induced Immunosuppression by Macrophages. Cell *175*, 442–457.e23.

54. Chen, G., Huang, A.C., Zhang, W., Zhang, G., Wu, M., Xu, W., Yu, Z., Yang, J., Wang, B., Sun, H., et al. (2018). Exosomal PD-L1 contributes to immunosuppression and is associated with anti-PD-1 response. Nature *560*, 382–386.

55. Dong, H., Strome, S.E., Salomao, D.R., Tamura, H., Hirano, F., Flies, D.B., Roche, P.C., Lu, J., Zhu, G., Tamada, K., et al. (2002). Tumor-associated B7-H1 promotes T-cell apoptosis: a potential mechanism of immune evasion. Nat. Med. *8*, 793–800.

56. Chen, L., and Han, X. (2015). Anti-PD-1/PD-L1 therapy of human cancer: past, present, and future. J. Clin. Invest. *125*, 3384–3391.

57. Shin, D.S., Zaretsky, J.M., Escuin-Ordinas, H., Garcia-Diaz, A., Hu-Lieskovan, S., Kalbasi, A., Grasso, C.S., Hugo, W., Sandoval, S., Torrejon, D.Y., et al. (2017). Primary Resistance to PD-1 Blockade Mediated by JAK1/2 Mutations. Cancer Discov. *7*, 188–201.

58. Patel, S.J., Sanjana, N.E., Kishton, R.J., Eidizadeh, A., Vodnala, S.K., Cam, M., Gartner, J.J., Jia, L., Steinberg, S.M., Yamamoto, T.N., et al. (2017). Identification of essential genes for cancer immunotherapy. Nature *548*, 537–542.

59. Deng, M., Gui, X., Kim, J., Xie, L., Chen, W., Li, Z., He, L., Chen, Y., Chen, H., Luo, W., et al. (2018). LILRB4 signalling in leukaemia cells mediates T cell suppression and tumour infiltration. Nature *562*, 605–609.

60. Cai, Z., Zhang, M.X., Tang, Z., Zhang, Q., Ye, J., Xiong, T.C., Zhang, Z.D., and Zhong, B. (2020). USP22 promotes IRF3 nuclear translocation and antiviral responses by deubiquitinating the importin protein KPNA2. J. Exp. Med. *217*, e20191174.

61. Kammertoens, T., Friese, C., Arina, A., Idel, C., Briesemeister, D., Rothe, M., Ivanov, A., Szymborska, A., Patone, G., Kunz, S., et al. (2017). Tumour ischaemia by interferon-γ resembles physiological blood vessel regression. Nature *545*, 98–102.

62. González-Navajas, J.M., Lee, J., David, M., and Raz, E. (2012). Immunomodulatory functions of type I interferons. Nat. Rev. Immunol. *12*, 125–135.

63. Yang, X., Zhang, X., Fu, M.L., Weichselbaum, R.R., Gajewski, T.F., Guo, Y., and Fu, Y.X. (2014). Targeting the tumor microenvironment with interferon-β bridges innate and adaptive immune responses. Cancer Cell *25*, 37–48.

64. Lawson, K.A., Sousa, C.M., Zhang, X., Kim, E., Akthar, R., Caumanns, J.J., Yao, Y., Mikolajewicz, N., Ross, C., Brown, K.R., et al. (2020). Functional genomic landscape of cancer-intrinsic evasion of killing by T cells. Nature *586*, 120–126.

65. Han, K., Pierce, S.E., Li, A., Spees, K., Anderson, G.R., Seoane, J.A., Lo, Y.H., Dubreuil, M., Olivas, M., Kamber, R.A., et al. (2020). CRISPR screens in cancer spheroids identify 3D growth-specific vulnerabilities. Nature *580*, 136–141.

66. Nagarajan, S., Rao, S.V., Sutton, J., Cheeseman, D., Dunn, S., Papachristou, E.K., Prada, J.G., Couturier, D.L., Kumar, S., Kishore, K., et al. (2020). ARID1A influences HDAC1/BRD4 activity, intrinsic proliferative capacity and breast cancer treatment response. Nat. Genet. *52*, 187–197.

67. Gao, P., Xia, J.H., Sipeky, C., Dong, X.M., Zhang, Q., Yang, Y., Zhang, P., Cruz, S.P., Zhang, K., Zhu, J., et al.; PRACTICAL Consortium (2018). Biology and Clinical Implications of the 19q13 Aggressive Prostate Cancer Susceptibility Locus. Cell *174*, 576–589.e18.

68. Bester, A.C., Lee, J.D., Chavez, A., Lee, Y.R., Nachmani, D., Vora, S., Victor, J., Sauvageau, M., Monteleone, E., Rinn, J.L., et al. (2018). An Integrated Genome-wide CRISPRa Approach to Functionalize lncRNAs in Drug Resistance. Cell *173*, 649–664.e20.

69. Chen, S., Sanjana, N.E., Zheng, K., Shalem, O., Lee, K., Shi, X., Scott, D.A., Song, J., Pan, J.Q., Weissleder, R., et al. (2015). Genome-wide CRISPR screen in a mouse model of tumor growth and metastasis. Cell *160*, 1246–1260.

70. Topalian, S.L., Solomon, D., and Rosenberg, S.A. (1989). Tumor-specific cytolysis by lymphocytes infiltrating human melanomas. J. Immunol. *142*, 3714–3725.

71. Yeh, H.M., Yu, C.Y., Yang, H.C., Ko, S.H., Liao, C.L., and Lin, Y.L. (2013). Ubiquitin-specific protease 13 regulates IFN signaling by stabilizing STAT1. J. Immunol. *191*, 3328–3336.

72. Dupont, S., Mamidi, A., Cordenonsi, M., Montagner, M., Zacchigna, L., Adorno, M., Martello, G., Stinchfield, M.J., Soligo, S., Morsut, L., et al. (2009). FAM/USP9x, a deubiquitinating enzyme essential for TGFbeta signaling, controls Smad4 monoubiquitination. Cell *136*, 123–135.

73. Wu, Y., Wang, Y., Yang, X.H., Kang, T., Zhao, Y., Wang, C., Evers, B.M., and Zhou, B.P. (2013). The deubiquitinase USP28 stabilizes LSD1 and confers stem-cell-like traits to breast cancer cells. Cell Rep. *5*, 224–236.